Application of Friction Stir Processing (FSP) as a Cladding Method to Produce AA2024-AA1050 Multi-layer Sheets

A. Jaferi Salour, Z. Sadeghian* and B. Lotfi

Department of Materials Science and Engineering, Faculty of Engineering, Shahid Chamran University of Ahvaz, Ahvaz, Iran

ARTICLE INFO

ABSTRACT

Friction stir processing (FSP) was used as a cladding method for the fabrication of a AA2024 clad layer on a AA1050 sheet. Crossover multi pass FSP with 50% overlap was considered as the cladding method. Effects of the number of FSP passes and post heat treatment on the microstructure and properties of clad layers were evaluated. Microstructural evolutions during the FSP and heat treatment were investigated by field emission scanning electron microscopy (FESEM). The results showed that a defect free clad layer and a uniform metallurgical interface between the clad layer and base material can be achieved by the FSP. Moreover, clad layers exhibited higher hardness values in comparison to the base material. T4 Heat treatment of the FSPed samples resulted in comparatively high hardness values after natural aging. The highest hardness value of about 160 HV was achieved after heat treatment of the sample obtained from 3 intersecting FSP passes. Tensile strength of clad layers increased to 317 MPa after three intersecting FSP passes, compared to about 70 MPa of Al substrate.

1. Introduction

Aluminium and its alloys have been considered as prime materials for different applications such as transportation, building, packaging and sport industries. AA2024 is a well-known Al alloy recognised for its high fatigue performance and formability, high damage tolerance, and high durability. Hence it is widely used in aircraft applications, especially in fuselage skins [1]. The combination of the acceptable cost, low density, appropriate mechanical properties, structural integrity and ease of fabrication is attractive in every application [1-3]. However, it is often difficult to attain a wide variety of requirements for a single material. To increase the persistence and performance, various methods have been developed to protect the components by distinctive coatings or clads. Coatings and clads of specific alloys and composites can provide a combination of various properties such as hardness and wear resistance on the surface and high toughness in the substrate in comparison with metal matrix composites (MMCs) or monolithic bulk materials [4].

Friction stir processing (FSP) is one of the techniques to fabricate surface composites and modify microstructural features. FSP has been derived from friction stir welding process and can be used for surface or in-volume processing of metals and alloys. This process has been recognized as an effective treatment for achieving microstructural refinement, densification and homogenization, as well as eliminating defects in castings and forgings [5-7].

* Corresponding author
  E-mail address: z.sadeghian@scu.ac.ir (Z. Sadeghian)

In FSP, a rotating tool that includes a shoulder and a pin is plunged into the surface of the material. Tool rotation creates frictional heat and the dynamic mixing of the metal underneath, which results in microstructural refinement and the incorporation and/or dispersion of the reinforcing particles into a matrix such as aluminium alloys, magnesium alloys and copper [8-9].

According to the literature, many researches have been involved in the butt and single seam lap joint configurations processed by FSW/FSP [10-11]. Recently, few attempts have been made to develop FSP/FSW as an alternative cladding technique, based on multi-seam friction stir lap welding. It has been reported that FSP/FSW can result in enhanced joint properties and reduced physical and metallurgical deficiencies in comparison with conventional cladding processes. An introductory study on the fabrication of AZ80/Al composite plate by the FSP was reported by Liu et al who indicated the formation of a dense composite Al layer with fine and uniform grains [12]. Lakshminarayanan and Annamalai studied the effects of the process parameters on the quality characteristics of dissimilar magnesium-aluminium alloy clad joints [13]. To the authors' knowledge, using intersecting passes for the FSP cladding has not been presented in the literature before. The effects of the overlapping multi-passes in two directions on the mechanical properties and microstructure of AZ31 magnesium alloy were studied, and it was indicated that two this directional overlap results in a decreased grain size and increased uniformity of the grain distribution, hardness, yield strength, and ultimate strength [14].

The aim of the present study was to fabricate a clad layer of AA2024 alloy on the surface of AA1050 alloy. Three intersecting passes were applied by the FSP to provide bonding between the two Al alloy sheets. The microstructure of the FSPed clad layers was studied by optical microscopy and scanning electron microscopy. Hardness profiles of the claddings were obtained from hardness measurements, and the tensile properties of the clad layers at ambient temperature were studied by tensile tests.

2. Experimental Details

Commercially pure Al alloy (AA 1050) was used as the base material. Rolled sheets of 8 mm thickness were cut to 140 mm× 140 mm specimens. AA 2024-T3 Al alloy with a thickness of 2 mm and 140 mm×140 mm area was considered as the cladding material. Chemical compositions of base and clad materials are presented in Table 1. Al2024 sheets were annealed at 380 ºC for two hours, before the FSP.

Table 1: Chemical composition of as-received AA1050 substrate and AA2024 clad layer.

Material	Al	Ti	Zn	Cr	Mg	Mn	Cu	Fe	Si
AA1050	99.7	0.006	0.005	0.001	--	0.001	0.001	0.17	0.048
AA2024	93	0.03	0.021	0.002	1.4	0.51	4.75	0.132	0.059

A milling machine (X52, Beijing No. 2 Machine Tool Works Co., Ltd.) was used to conduct the FSP experiments. A cylindrical threaded tool containing a pin of 6 mm diameter and 5 mm length, and a shoulder of 18 mm diameter made of hot worked H13 tool steel was used for the FSP. The tool was hardened to achieve a hardness of 53 HRC. Tool rotational speed of 1000 rpm with traverse speed of 40 mm/min at 2.5º tilt angle were used for FSP cladding. The AA 2024 cladding sheet was overlaid on a AA 1050 substrate and fixed firmly by jigs. FSP Cladding was conducted by three intersecting FSP passes of about 50% overlap as shown in (fig. 1).
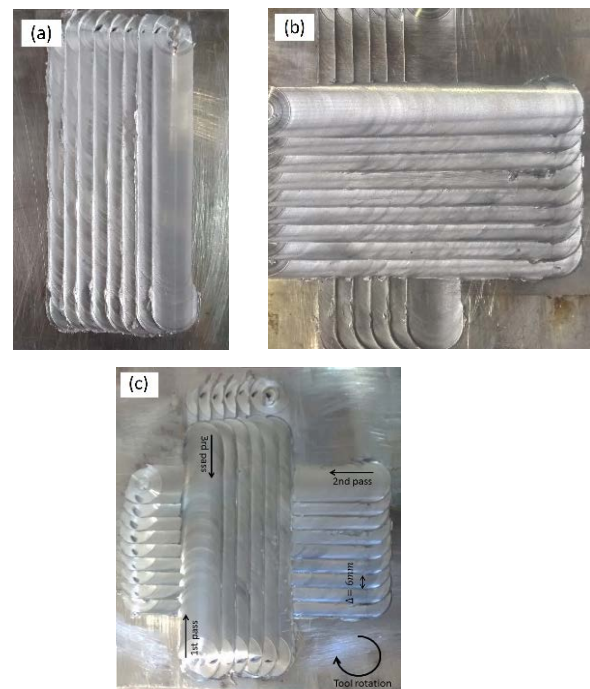

Fig. 1. Typical surface appearance of the FSPed samples after the a) first pass, b) second cross over, and c) third intersectional passes

The FSPed samples were heat treated with T4 conditions (solution treatment at 480 °C for 1 h, water quenched to room temperature and naturally aged). The FSP cladded samples were sectioned and prepared by metallographic techniques for microstructural investigations. A Mira3 Tescan field emission scanning electron microscope (FESEM) was used for the microstructural investigation of the cross sections of the samples. Samples for microstructural testing were cut perpendicular to the direction of the latest FSP pass. Vickers microhardness tests were carried out on the FSP substrate and cladded samples before and after T4 heat treatment to achieve cross sectional microhardness profiles along the clad layer and from the FSPed 2024 clad layer to the base material. Microhardness measurements were performed using a Nexus Innova 4300 microhardness testing machine under 100 g loading for 10 seconds. Tensile properties were determined by a SANTAM-STM-50KN machine according to the ASTM E8M standard [15]. Flat tensile specimens of 6.4 mm gauge length, 2.5 mm width and 1.5 mm thickness were machined out from the AA1050 base material and clad layers parallel to the latest FSP pass. Tensile experiments were conducted at ambient temperature with a strain rate of 10^{-3} s^{-1}. A schematic illustration of the metallography and tensile test specimens is presented in (Fig. 2).
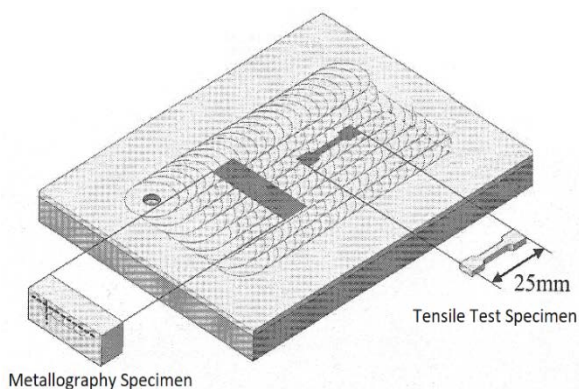

Fig. 2. schematic illustration of the metallography and tensile test specimens according to the direction of the last FSP pass

3. Results and Discussion

Figure 2 shows the cross-sectional SEM micrographs of the cladded samples after different FSP passes. The resultant clad layers seem to be free of microstructural defects such as tunnels and worm holes after three FSP passes. This can be attributed to the sufficient stirring of the material during the FSP as a result of the optimum combination of the process parameters [8]. It should be mentioned that other combinations of the FSP parameters could not result in flawless samples. As shown in (Fig. 2a), AA2024 was cladded successfully on the surface of the Al substrate, even after the first FSP pass. However, a few flaws can be seen in the clad layer obtained from one FSP pass. The height of the stir zone seems to be about 5 mm which is equal to the length of the pin. Considering the thickness of AA2024 cladded sheet (2 mm), it can be suggested that both clad and substrate have been affected by the stirring effect of the FSP. After the second FSP pass (intersectional direction), a more uniform stir zone can be seen with no significant difference in the thickness compared to that obtained from the first pass, as shown in (Fig. 2b). The sample obtained from three intersecting FSP passes showed the most uniform AA2024 clad layer without any apparent defects. Considering the advancing side (AS) and the retreating side (RS) for each FSP pass, shown in (Fig. 1c), the waviness of the clad surface can be explained. On the surface of the clad layers obtained from one and two FSP passes a somehow waved surface with curling flashes can be seen.

Overlapped by the AS, a pronounced waved surface is produced since the flashes are actually curling over the previous pass, giving a wavelike finishing to the surface. This feature has been changed after three FSP passes. In the clad layer obtained from the third FSP pass, AS and RS sides are opposing those of the first pass and this could result in a smoother surface finish by the successive destruction of the flashes on the AS of the two previous passes. Gandra et al. reported similar results after investigating the effect of the overlapping direction during the FSP [16].
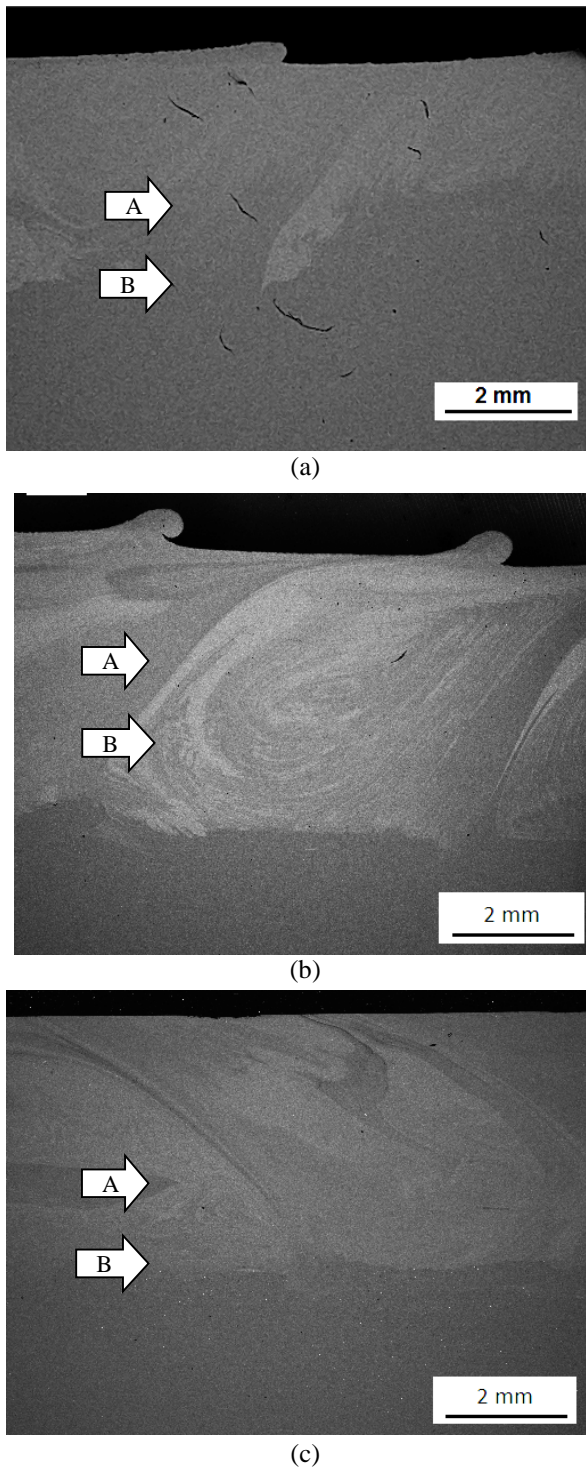
(a)

(b)

(c)

Fig. 3. SEM cross-sectional images of the FSPed AA2024 clad layers on the AA1050 obtained from a) one, b) two and c) three FSP passes.

Figure 3 shows distinct regions of the clad layers obtained from different FSP passes, which are also shown in (Fig. 2). Zone A is about 2 mm under the surface of all the FSPed samples which can be considered as the initial interface between AA2024

sheet and the substrate. Zone B demonstrates the bottom of the stir zone considering the height of the pin. As can be seen in the SEM micrographs, even in zone B, which is about 2 mm underneath the interface of the clad layer and the substrate, the precipitates belonging to AA2024 sheet have been dispersed. However, by increasing the number of the intersecting FSP passes, a more uniform distribution of the precipitates in zone B can be seen. It should be mentioned that the quantity of the precipitates in zone B is less than that in zone A.

Figure 4 shows the microhardness profiles of the AA2024 clad layers on the surface and across the layer after different FSP passes. The mean hardness of the clad layer obtained from the first FSP pass was about 80 HV and increased slightly to about 100 HV after applying the second intersecting FSP pass. It has been reported that during the FSP the material is affected by the annealing effect of the process, which can reduce the hardness as well as dynamic recrystallization that can reversely enhance it [17-19]. Therefore, in the present study, it can be concluded that the dynamic recrystallization may have been dominant compared to the annealing effect of the FSP. The same behaviour has been reported for AA6063-T6 [17, 20]. Hardness profiles of the FSPed samples from AA2024 clad layer to Al substrate showed an increase from about 25 HV in the substrate to a maximum of 100 HV on the surface of the clad layer. It should be noticed that the depth of the zone with increased hardness developed to more than 3 mm after the second FSP pass. Considering the thickness of AA2024 sheet (2 mm), it can be concluded that at the interface the clad layer was mixed with the substrate and this resulted in an increase in the hardness. This is in agreement with the SEM micrographs of the clad layers. After 3 FSP passes, no significant increase in the hardness was achieved. However, it is worth noticing that the hardness value dropped at some points compared to that obtained after 2 FSP passes. This may be explained by the local over aging of the precipitates due to a temperature rise during the FSP [21].
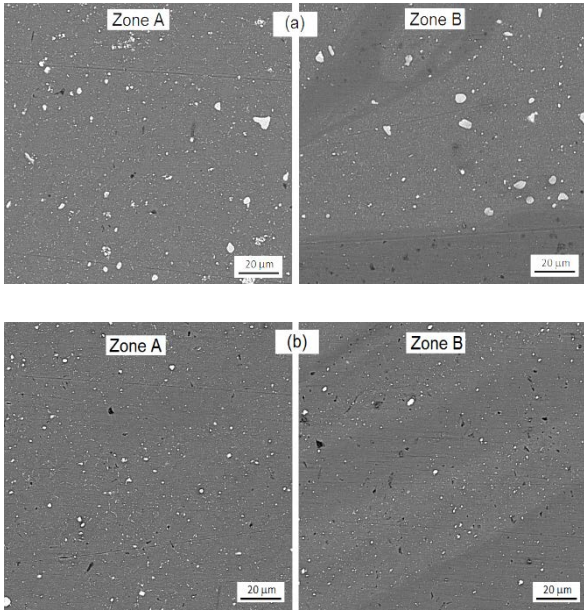
Fig. 4. Cross-sectional SEM micrographs of AA2024 clad layers at different zones depicted in Fig. 1 after a) one, b) two and c) three FSP passes.
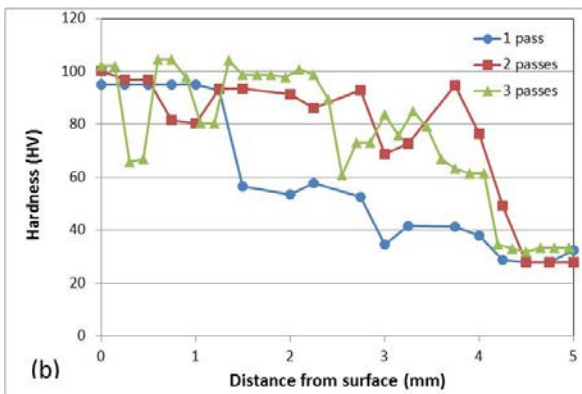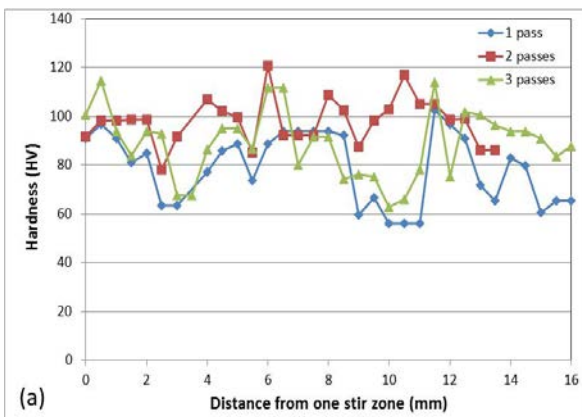

Fig. 5. Microhardness profiles of the FSPed AA2024 clad layers on Al substrate after different FSP passes; a) on the surface of clad layer and b) from the clad layer to the substrate.

The engineering stress-strain curves obtained from tensile experiments conducted on samples obtained from AA2024 clad layers after different FSP passes are shown in (Fig. 5). As can be observed all the FSPed clad layers show considerably higher yield and tensile strength compared to AA1050 substrate. It should be noted that increasing the number of the FSP passes also resulted in the improvement of the tensile properties. Enhancement of the mechanical properties due to the FSP has been attributed not only to the refining action of the microstructure induced by the dynamic recrystallization mechanisms during the process, but also to the elimination of the defects such as micro porosities or cracks [22]. The latter may be considered as the reason for simultaneously enhanced strength and ductility obtained from the sample produced by three intersecting FSP passes.
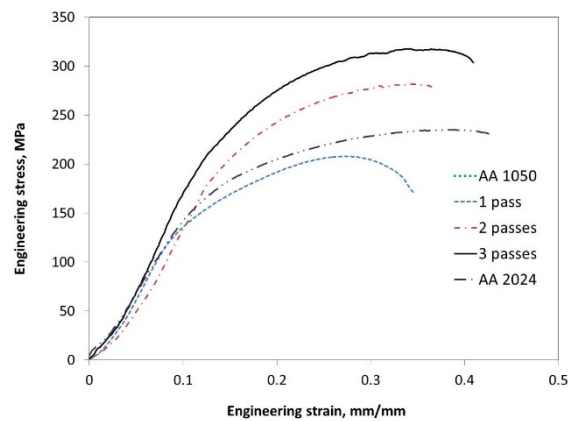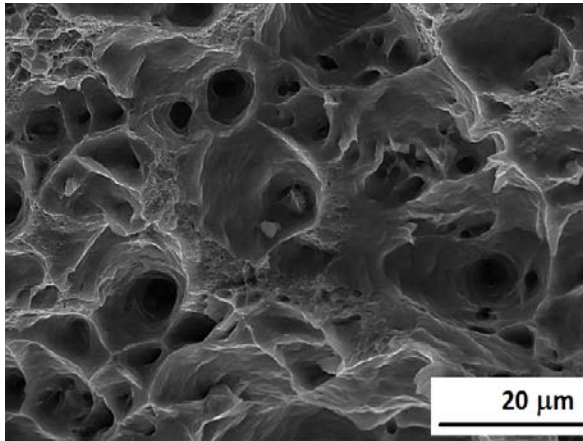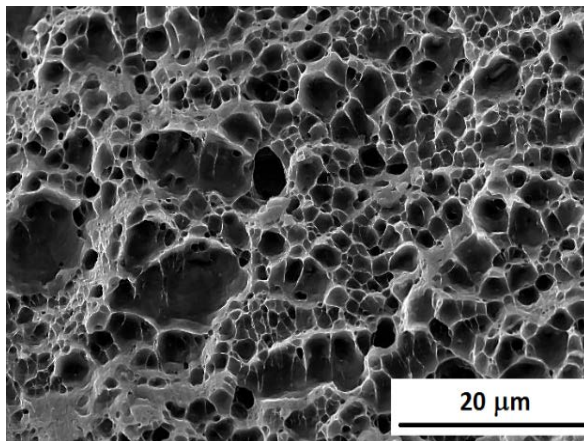

Fig. 6. Engineering stress strain curves obtained from the base material and AA2024 clad layers after different FSP passes.

Figure 6 indicates the SEM micrographs of the fracture surfaces of the FSPed samples. The fracture surface of AA1050 showed the typical ductile fracture mode with relatively large equiaxed dimples. AA2024 clad layer obtained from one FSP pass exhibited a bimodal dimple size in the fracture surface with a large number of small dimples (<3 μm) and a few scattered larger dimples up to about 10 μm. In the FSPed samples, failure occurs by the initiation of voids at triple junctions and sub-grain and/or grain boundaries. Meanwhile some voids may propagate through the weakest paths, such as the neighbouring sub-grain and/or grain boundaries and by their coalescence large dimples are formed. This feature can also be observed in the fracture surface of the clad layer obtained from two FSP passes (Fig. 5c). By
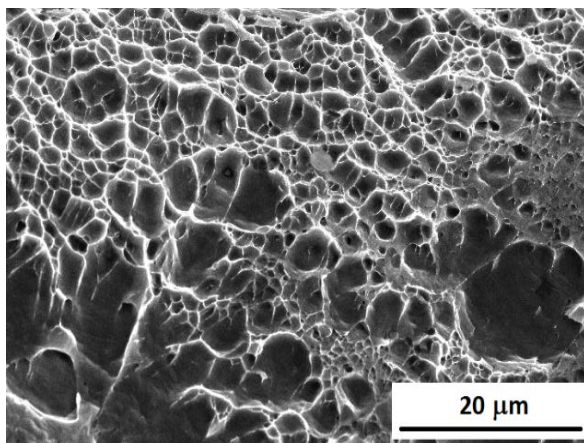
increasing the number of FSP passes to three, a relatively homogeneous distribution of very small and narrow dimples of about 1 μm can be observed in the SEM micrograph of the fracture surface. This can be related to the smaller grain size obtained after three FSP passes [17,23].
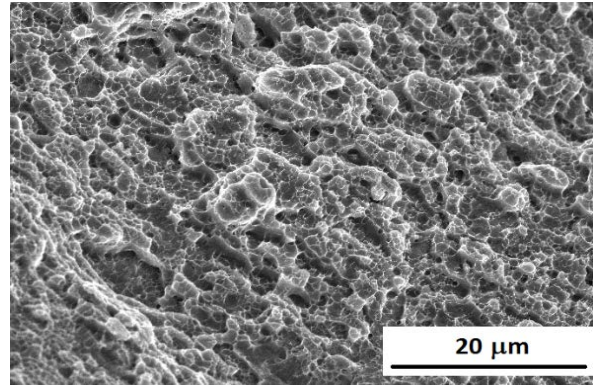
(a)

(b)

(c)

(d)

Fig. 6. Fracture surface SEM micrographs of a) AA1050, and AA2024 clad layers obtained from b) one, c) two, and d) three FSP passes.

Figure 7 shows the microhardness profiles on the surface and across AA2024 clad layers obtained from different FSP passes after T4 heat treatment. In comparison with (Fig. 4), it is evident that a significant increase in the microhardness occurred in the FSPed clad layers after T4 heat treatment. In the AA2024 clad layer obtained from three FSP passes, a hardness of up to 160 HV could be achieved on the surface after natural aging. Meanwhile, the FSPed sample obtained from three intersecting passes showed more uniform distribution of hardness values compared to other samples. It has been reported that the dissolution of coarse precipitates by solution annealing and re-precipitation of fine precipitates during aging is the reason for the increased hardness observed in the heat-treated samples [24]. FESEM micrographs of the T4 heat treated samples are shown in (Fig. 8). As can be observed, after T4 heat treatment the size of the precipitates in all samples has decreased significantly, compared to that of the FSPed samples. It is worth noting that the AA2024-T4 clad layer obtained from three intersecting FSP passes exhibited meaningful uniform distribution of smaller precipitates in comparison to other samples. This can be explained by the uniform distribution of the precipitates in this clad layer due to additional FSP passes (as seen in (Fig. 3c), which resulted in the enhanced dispersion of the elements during solution annealing, and more uniform re-precipitation of GP-Zones during natural aging. A similar phenomenon has been reported and explained by other researchers [24].
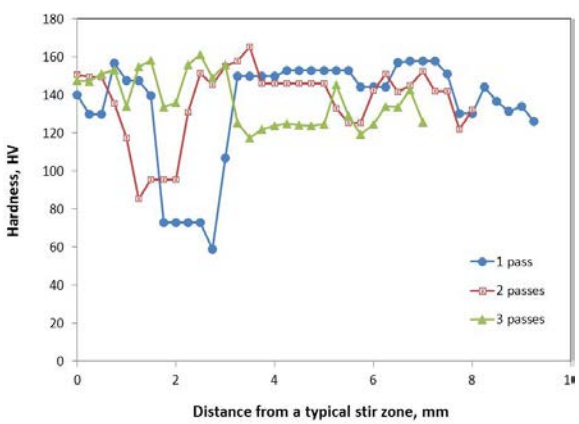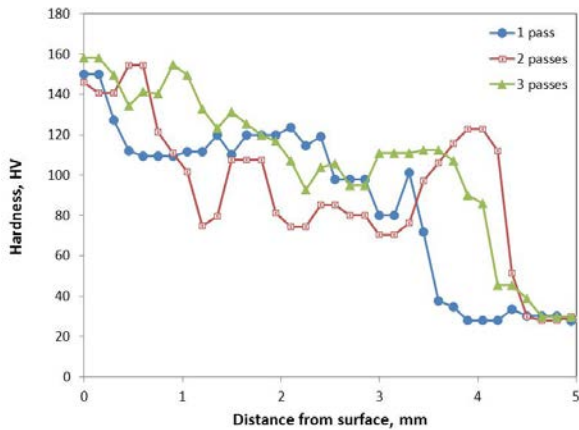
Fig. 7. Microhardness profiles of the T4- heat treated FSPed AA2024 clad layers on Al substrate after different FSP passes; a) on the surface of the clad layer and b) from the surface of the clad layer to the substrate.
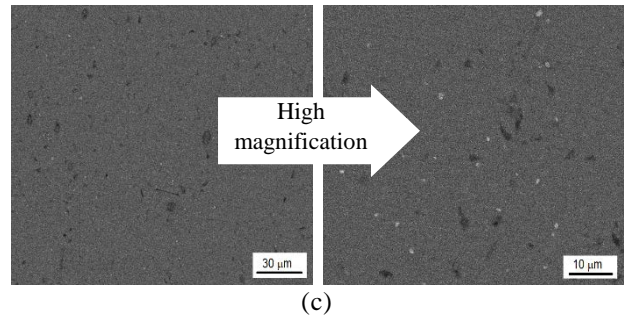

(a)

(b)

(c)

Fig. 8. Cross-sectional SEM micrographs of AA2024 clad layers after T4 heat treatment a) one, b) two and c) three FSP passes.

4. Conclusion

The FSP was successfully applied for the cladding of AA2024 alloy on AA1050 using three intersecting passes. Clad layers obtained from different FSP passes were sound and defect-free with a metallurgical clad-substrate interface. The hardness of the clad layer obtained from three intersecting FSP passes was about 100 HV compared to 25 HV of Al substrate, which increased to 160HV after T4 heat treatment. Tensile strength of 317 MPa was achieved in AA2024 clad layer compared to about 70 MPa of Al substrate.

5. Acknowledgement

6. References

[1] Z. Ahmad, Aluminium Alloys - New Trends in Fabrication and Applications, first edition, In Tech, United Kingdom, (2012) 48-97.

[2] P. Rambabu, N. Eswara Prasad, V.V. Kutumbarao, R.J.H. Wanhill, Aluminium Alloys for Aerospace Applications. In: Prasad N., Wanhill R. (eds) Aerospace Materials and Material Technologies. Indian Institute of Metals Series. Springer, Singapore, (2017) 29-52.

[3] F. Casarotto, A.J. Franke R. Franke, Advanced Materials in Automotive Engineering, edited by Jason Rowe, Woodhead Publishing, Cambridge, UK, 109 (2012).

[4] Sergio Correia, Vitor Anes, Luis Reis, Effect of surface treatment on adhesively bonded aluminium-aluminium joints regarding aeronautical structures, *Engineering Failure Analysis*, 84 (2018) 34-45.

[5] Y. Chi, G. Gu, H. Yu, C. Chen, Laser surface alloying on aluminum and its alloys: A review, *Optics and Lasers in Engineering*, 10**0** (2018) 23-37.

[6] W. Zhang, H. Ding, M. Cai, W. Yang, J. Li, Ultra-grain refinement and enhanced low-temperature superplasticity in a friction stir-processed Ti-6Al-4V alloy, *Materials Science and Engineering: A*, 727 (2018) 90-96.

[7] H. Eskandari, R. Taheri, F. Khodabakhshi, Friction-stir processing of an AA8026-TiB2-Al2O3 hybrid nanocomposite: Microstructural developments and mechanical properties, *Materials Science and Engineering: A*, 660 (2016) 84-96.

[8] M. Balakrishnan, I. Dinaharan, R. Palanivel, R. Sathiskumar, Effect of friction stir processing on microstructure and tensile behavior of AA6061/Al3Fe cast aluminum matrix composites, *Journal of Alloys and Compounds* (2019) in press, https://doi.org/10.1016/j.jallcom.2019.01.211.

[9] Z. Ma, Friction Stir Processing Technology: A Review, *Metallurgical and Materials Transactions A*, 39(3) (2008) 642-658.

[10] O.S. Salih, H. Ou, W. Sun, D.G. McCartney, A review of friction stir welding of aluminium matrix composites, *Materials & Design*, 86 (2015) 61-71.

[11] G. Buffa, D. Baffari, A. Di Caro, L. Frantini, Friction stir welding of dissimilar aluminium–magnesium joints: Sheet mutual position effects, *Science and Technology of Welding and Joining*, 20 (2015) 271−279.

[12] Y. Yong, Z. Da-tong, Q. Cheng, Z. Wen, Dissimilar friction stir welding between 5052 aluminum alloy and AZ31 magnesium alloy, *Transactions of Nonferrous Metals Society of China*, 20 (2010) 619−623.

[13] F. Liu, Q. Liu, C. Huang, K. Yang, C. Yang, L. Ke, Microstructure and corrosion resistance of AZ80/Al composite plate fabricated by friction stir processing, *Material Science Forum*, 747−748 (2013) 313−319.

[14] A.K. Lakshminarayanan, V.E. Annamalai, Fabrication and performance evaluation of dissimilar magnesium–aluminium alloy multi-seam friction stir clad joints, *Transactions of Nonferrous Metals Society of China*, 27(1) (2017) 25-35.

[15] A. Alavi Nia, H. Omidvar, S.H. Nourbakhsh, Effects of an overlapping multi-pass friction stir process and rapid cooling on the mechanical properties and microstructure of AZ31 magnesium alloy, *Materials and Design*, 58 (2014) 298-304.

[16] Standard test methods for tension testing of metallic materials, ASTM International, (2010).

[17] J. Gandra, R.M. Miranda, P. Vilaça, Effect of overlapping direction in multi-pass friction stir processing, *Materials Science and Engineering: A*, 528 (16–17) (2011) 5592-5599.

[18] T.R. McNelley, S. Swaminathan, J.Q. Su, Recrystallization mechanisms during friction stir welding/processing of aluminum alloys, *Scripta Materialia*, 58 (5) (2008) 349-354.

[19] L. John Baruch, R. Raju, V. Balasubramanian, A. G. Rao, I. Dinaharan, Influence of Multi-pass Friction Stir Processing on Microstructure and Mechanical Properties of Die Cast Al–7Si–3Cu Aluminum Alloy, *Acta Metallurgica Sinica (English Letters)*, 29(5) (2016) 431-440.

[20] K.V. Jata, S.L. Semiatin, Continuous dynamic recrystallization during friction stir welding of high strength aluminum alloys, *Scripta Materialia*, 43 (2000) 743-749.

[21] N. Nadammal, S.V. Kailas, J. Szpunar, S. Suwas, Restoration Mechanisms During the Friction Stir Processing of Aluminum Alloys, *Metallurgical and Materials Transactions A,* 46 (7) (2015) 2823-2828.

[22] M.L. Santella, T. Engstrom, D. Storjohann, T.Y. Pan, Effects of friction stir processing on mechanical properties of the cast aluminum alloys A319 and A356, Scripta Materialia, 53 (2) (2005) 201-206.

[23] A. Kumar, S.K. Sharma, K. Pal, S. Mula, Effect of Process Parameters on Microstructural Evolution, Mechanical Properties and Corrosion Behavior of Friction Stir Processed Al 7075 Alloy, *Journal of Materials Engineering and Performance*, 26 (3) (2017) 1122-1134.

[24] D. M. Sekban, S. M. Aktarer, H. Shang, P. Xue, Z. Ma, G. Purcek, Microstructural and Mechanical Evolution of a Low Carbon Steel by Friction Stir Processing, *Metallurgical and Materials Transactions A*, 48 (2017) 3869-3879.

[25] D. Ghanbari, M. Kasiri Asgarani, K. Amini, F. Gharavi, Influence of heat treatment on mechanical properties and microstructure of the Al2024/SiC composite produced by multi–pass friction stir processing, *Measurement*, 104 (2017) 151-158.

استفاده از فرایند اصطکاکی اغتشاشی (FSP) به عنوان روش روکش‌کاری برای تولید ورق‌های چندلایه AA2024-AA1050

امین جافری‌سالور، زهره صادقیان و بهنام لطفی

گروه مهندسی مواد، دانشکده مهندسی، دانشگاه شهید چمران اهواز، اهواز، ایران.

چکیــــده

فرایند اصطکاکی اغتشاشی (FSP) به عنوان روش روکش‌کاری برای تولید لایه روکش AA2024 روی ورق AA1050 استفاده شد. پاس‌های تقاطعی FSP با همپوشانی ۵۰٪ برا ی روکش‌کاری درنظر گرفته شد. تأثیر پاس‌های FSP و عملیات حرارتی بعدی بر ریزساختار و خواص روکش‌ها ارزیابی شد. تغییرات ریزساختاری حین FSP و پس از عملیات حرارتی با استفاده از میکروسکوپ الکترونی انتشارمیدانی (FESEM) بررسی شد. نتایج نشان داد که روکش بدون عیب با فصل مشترک یکنواخت متالورژیکی با استفاده از فرایند FSP قابل دستیابی است. به‌علاوه، لایه‌های روکش مقادیر بالاتر سختی نسبت به ماده پایه نشان دادند. عملیات حرارتی T4 برروی نمونه‌های FSP شده منجر به سختی بالاتری پس از پیرشدن طبیعی گردید. مقدار سختی ۱۶۰ ویکرز پس از عملیات حرارتی نمونه حاصل از سه پاس تقاطعی به‌دست آمد. استحکام کششی لایه‌های روکش در مقایسه با استحکام ۷۰ MPa در فلز پایه تا ۳۱۷ MPa پس از سه پاس تقاطعی افزایش یافت.

واژه‌های کلیدی: روکش‌کاری، فرایند اصطکاکی اغتشاشی، AA 2024